Desalination and Water Treatment
www.deswater.com

doi: 10.5004/dwt.2020.26264

204 (2020) 164–173
November

Artificial neural network and genetic algorithm for modeling and optimization of photocatalytic removal of aquatic dye by g-C_3N_4/N-TiO_2 nanoparticles

Samira Taherkhani[a], Leila Ghalamchi[b], Farzaneh Mohammadi[c,*]

[a]*Applied Chemistry Research Laboratory, Department of Chemistry, Faculty of Science, University of Zanjan, Zanjan, Iran*
[b]*Research Laboratory of Environmental Protection Technology (RLEPT), Department of Applied Chemistry, Faculty of Chemistry, University of Tabriz*
[c]*School of Health, Isfahan University of Medical Sciences, Isfahan 81746-73461, Iran, Tel. +98 9134733362; email: fm_1363@hlth.mui.ac.ir (F. Mohammadi)*

Received 25 January 2020; Accepted 12 June 2020

ABSTRACT

Herein, we report the modification of nitrogen-doped TiO_2 (N-TiO_2) photocatalytic activity with graphite-like carbon nitride (g-C_3N_4). Also, the photo-degradation performance of Reactive Orange 122 (RO122) was investigated under visible light irradiation. The UV-vis spectrophotometer revealed that the absorption edge of nanocomposite was shifted to the lower energy, as compared with only N-TiO_2 nanoparticles. The visible light induced the photocatalytic activity of N-TiO_2/g-C_3N_4 nanoparticles; they were significantly increased by combining N-TiO_2 with g-C_3N_4 nanosheets. The effects of some key factors including pH, dye concentration, catalyst dosage, and reaction time on the photocatalysis removal process of RO122 were also evaluated. Artificial neural network model hybridized with the genetic algorithm (ANN-GA) strategy was proposed to model and optimize the photocatalytic degradation of RO122 in a batch system. The results showed that the photocatalytic process could be well predicted by ANN, using 4:20:1 topology. The genetic algorithm was also utilized to optimize the model conditions of the input parameters. The ANN-GA method was capable of effectively modeling and optimizing the photocatalytic efficiency of the prepared N-TiO_2/g-C_3N_4 nanocomposite under visible light.

Keywords: Genetic algorithms; Artificial neural network; Carbon graphite nitride; Modeling; Titanium oxide

1. Introduction

Nowadays, due to the problems of environment contamination and lack of the energy, research has been concerned with water and wastewater treatment [1–3]. Also, discharge of pollutants such as EDCs, pesticides, drugs, dyes, etc., from various sources, especially different industries, causes environmental pollution, which is a serious concern [4]. Because of the dyes toxicity, it is essential to eliminate them from wastewater before discharging to environment. Several biological and physico-chemical treatment processes such as ion exchange, Fenton's reagent, aerobic and anaerobic bioremediation, ozonation, oxidative process, electrochemical destruction, electro kinetic coagulation, membrane filtration, and adsorption have already been applied for the removal of dyes from wastewater [5,6]. Advanced oxidation processes (AOPs) have been applied as one of the emerging wastewater decontamination technologies for the management of recalcitrant micropollutants [7,8]. Photocatalysis process, as a subset of AOPs, has been widely researched, receiving great attraction since the past decades. TiO_2 has been identified as a highly efficient photocatalyst because of its nontoxic property, high chemical stability, and excellent energy conversion efficiency, as well as acting as a photo-stable semiconductor with a high band energy (E_{bg} = 3.0–3.2 eV) owing to its activity in the ultraviolet

* Corresponding author.

region [9–13]. Developing new photocatalysts with high photogenerated charge separation and wide response wavelength range is, therefore, a key issue for researches. By tailoring TiO_2 with some noble metals and non-metals, the catalytic activity of it can be increased. To increase the photo responding range into visible light, the use of nitrogen-doped atoms as the non-metal dopant into TiO_2 can shift the adsorption edge to the visible light [14–16]. According to the previous studies, the bond gap energy of TiO_2 can be diminished from 3.18 to 2.20 eV by nitrogen incorporation. Recently, graphite-like carbon nitride (g-C_3N_4), as a metal-free and n-type semiconductor, has been introduced as another highly efficient photocatalyst. Due to the special structure of g-C_3N_4, it is stable under light irradiation and in the pH value range of 0–14. This photocatalyst is widely used for lots of applications such as CO_2 reduction, hydrogen evolution and wastewater treatment because of its low cost and high chemical stability [17]. Moreover, the lower band gap (2.73 eV) of g-C_3N_4, as compared with TiO_2, represents the g-C_3N_4 response wavelength up to 450 nm [18]. However, the photodegradation of the pure g-C_3N_4 is limited due to the fast recombination of its electron-hole pairs [19]. It is noteworthy that combining g-C_3N_4 with N-TiO_2 can improve the separation rate of photogenerated carriers and enhance the quantum yield. In the present work, firstly, g-C_3N_4/N-TiO_2 nanocomposite as a photocatalyst was synthesized due to the increase in the photocatalytic ability of TiO_2 and inhibition of the electron-hole pair recombination in visible irradiation. The removal of the reactive orange 122 (RO122) from the aqueous solution was also studied to investigate the photocatalytic efficiency of g-C_3N_4/N-TiO_2. Then, some effective parameters including pH, catalyst dosage, and dye concentration were also investigated. In recent years, computer simulations have been widely used in solving environmental problems [20]. Artificial neural network (ANN) techniques can be regarded as a good alternative to traditional models because this method has a high potential in the interpretation of nonlinear and complex relations between variables [21]. Over the past decade, ANN models have been introduced in various fields of environmental engineering [22,23]. The neural network applications are such as: modeling and optimization of the photocatalytic ozonation of ciprofloxacin in aqueous solutions using TiO_2/MMT nanocomposite by ANN and the genetic algorithm [24]. A review of ANNs used for adsorption of dyes from the aqueous solution [5]. Moreover, in other reports, modeling, and optimization of sludge bulking in the wastewater treatment plant using ANN [25]. The use of neural networks and genetic algorithms to predict water quality [26]. Dioxin emission modeling from solid waste incinerators using neural networks [27]. Also, ANN has been applied for modeling and studying variables affecting the photocatalysis process by introducing mathematical functions for both linear and non-linear systems [21]. There are various researches using ANN to get experimental information regarding the model design of water and waste water treatment processes [28–31]. Genetic algorithm (GA), an evolutionary algorithm-based methodology, is applied to find the exact solutions for the optimization of the parameters [32].

The use of ANN and GA has been reported for the modeling and optimization of the landfill leachate photocatalytic treatment with the application of the tungsten-doped TiO_2 nano photocatalysts. The effect of four parameters (tungsten content, pH, leachate exposure time, and calcination temperature) was investigated on the process efficiency [33]. In another work, Khajeh et al. [34] developed an ANN model and optimized it by GA for the determination of methylene blue adsorption usage of wood sawdust as an adsorbent from the aqueous samples. The temperature, pH, time, and amount of the adsorbent were applied as the input variables, and the removal percentage of methylene blue was considered as the ANN output. The results of these studies have demonstrated the good ability of ANN and the GA in predicting and optimizing the performance of the treatment process.

Here, the ANN model was designed to predict the performance of the photocatalytic removal of the aquatic dye by g-C_3N_4/N-TiO_2 nanoparticles; therefore, an ANN model was applied to predict the removal efficiency by the statistic processes of 630 experimental data. Finally, the optimal condition was obtained using GA. Based on the trained model, the seven key process operating variables were optimized by the GA method. The experimental and corresponding simulate results were also compared. To the best of author's knowledge, there are no other reports in the literature regarding the modeling of RO122 removal by using the visible light photocatalyst, g-C_3N_4/N-TiO_2.

2. Materials and method

2.1. ANN theory

ANNs are an information processing system and computational models inspired by the brain's nerve cells function. The development of the ANN is meant to compute the output variables of a process with the help of input variables and calculations within the network [35].

The neural network is trained to recognize a specific function. For training, the output values predicted by the model are compared with the target vector that is the experimental results. Correcting connections values (weights) between the elements is done with the calculation of the error value. This will continue as long as the good predictive ability of the network is achieved and the model outputs have a good compliance with the targeted vector. Fig. 1a shows these concepts.

Trained ANNs are applied to perform complex algorithms and functions in different issues, including classification, pattern recognition, character recognition, vision, identification, and control systems. Various types of training algorithms have been applied for solving complex and nonlinear problems. Back propagation is one of the most popular types of training algorithms used for feed forward neural networks (FFNNs) [36]. The base component of neural networks is neuron or node, as shown in Fig. 1b.

Input and output variables are shown, respectively, with a_1–a_n and O_j. Each node receives many signals and neuron investigates them, making an output signal. W_{1j}–W_{nj} are the weights given to the inputs of each neuron. Weights are the adaptive factors in the neural network that define the input parameters intensity for the neuron. Each input (a_1, a_2,..., a_n) is multiplied by their respective weight (W_1, W_2,..., W_n), and

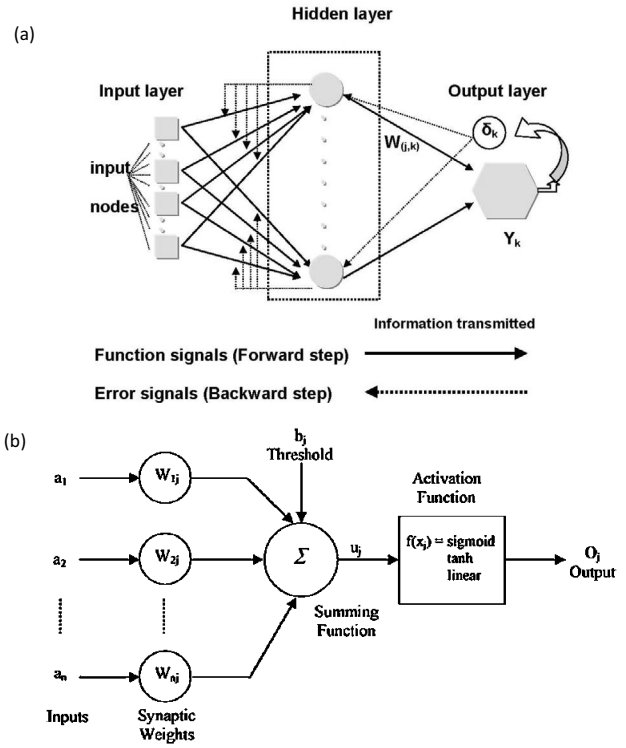

Fig. 1. (a) Neural networks training structure and (b) structure of a neural network neuron.

all of these values are added together ($a_1 \times W_1 + a_2 \times W_2 + ... + a_n \times W_n$); then, the transfer function estimates the output signal. Another input to node is b_j, that is called the internal threshold or bias. This is a randomly selected value making the outputs more accurate. Eq. (1) expresses the mentioned operations.

$$u_j = \sum_{i=1}^{n}\left(W_{ij} \times a_i\right) + b_j \tag{1}$$

The final output of nodes (O_j) is obtained with a mathematical operation on u_j. This is defined as the transfer function that changes u_j into O_j by the linear or nonlinear behaviour. Common transfer functions are expressed in the following equations [20].

- Sigmoid transfer function

$$f(x) = \frac{1}{1+e^{-x}} \qquad 0 \le f(x) \le 1 \tag{2}$$

- Hyperbolic tangent transfer function

$$f(x) = \tanh(x) = \frac{e^{x} - e^{-x}}{e^{x} + e^{-x}} \qquad -1 \le f(x) \le +1 \tag{3}$$

- Linear transfer function

$$f(x) = x \quad -\infty < f(x) < +\infty \tag{4}$$

2.2. Theory of genetic algorithm

Genetic algorithm is basically a search heuristic technique inspired by the process of natural selection. The development basis of this method is Darwin's theory of evolution. At first, genetic algorithms were developed by John Holland as a tool to find the best solutions for the complex issues. This procedure is implemented by creating a population of chromosomes. Then the people in the population are put at the control of the evolution process. Each evolutionary step is named generation and every member of the population is evaluated on the basis of a series of pre-defined quality criteria. This is done by a fitness function. For the next generation, people are chosen on the basis of their competence. So, the more qualified individuals are selected several times for the new population and they will have more chances to reproduce, whereas less qualified people are faded, with no chance for selection and reproduction. So, the more deserving chromosomes are increased until one of the stopping criteria is fulfilled. At this stage, the best solution is achieved [37].

In GA, A chromosome is a set of variables (parameters) in a string form defining a suggested solution to the Issue. The quality of a chromosome is evaluated by the fitness function as a response to the problem. GA component selection is done so that the chromosomes can be directed to evolution. The recombination is a process in which the competent chromosomes are selected; they are called parent and the next generation is produced from them. The main components of the recombination are crossover and mutation. Crossover is conducted through the exchange of parts of chromosome of two parents; so, one or two new members are created; they are called children. Mutation acts on a single chromosome and by changing chromosome components, the new members are produced. The stopping criteria are determined according to the number of the produced generations or the desired competencies [38].

2.3. Data collection

The subject of research, reactive orange, was actually taken from Boyakhsaz Co., Iran, as shown in Table 1. Titanium dioxide P-25, with the characteristics of Anatase/Rutile phases and the 80/20 ratio, the particle size of around 25 nm, and the surface area of 55 ± 15 m^2/g, was obtained from Degussa–Evonik Co. Chemicals such as sodium hydroxide (98%), nitric acid (65% by weight), ethanol, (99.5%) were all supplied by Merck (Darmstadt, Germany). Deionized water was used to prepare the desired concentration of the catalyst and dye solutions.

A Pyrex photoreactor was employed for the experiments; so different intensities of visible light sources were set to 15 cm above the photocatalyst surface. The UV-vis spectrophotometer (DR 5000, Hach, USA) was used to analyze the concentration of the dye in a clean transparent solution. As well, MATLAB was used to realize the genetic algorithm and run the ANN by the use of M-file script programming in the Microsoft Windows XP environment.

2.4. Synthesis of g-C_3N_4/N-TiO_2 nanocomposite

Direct heating of melamine precursor was the first step in the preparation of the bulk g-C_3N_4 [31]. For this purpose,

Table 1
Features of designated neural network

Network inputs	Initial concentration, photocatalyst dosage, pH, and contact time
Network outputs	Removal efficiency
Network type	Feed-forward back-propagation (FFBP)
Training function	trainscg
Adaption learning function	LEARNGDM
Performance function	MSE, R
Number of layers	20
Number of neurons in hidden layers	10–20
Transfer function	In hidden layer: sigmoid In output layer: sigmoid

an absolute amount of melamine was dried in an oven at 80°C for 3 h to make a dried powder put in a muffle furnace and Ar gas atmosphere at 520°C for 2 h. The g-C_3N_4 nanosheet was synthesized by heating 2 g of the bulk g-C_3N_4 at 520°C in the presence of oxygen. Ethanol was used to wash the prepared powder three times. Nitrogen doping in the commercial TiO_2 would cause the preparation of N-TiO_2 in the mechanical mixing of 0.8 g urea as the nitrogen source and 0.2 g TiO_2 P25. The mixture was heated to 450°C by the heating rate of 4°C/min for 4 h. Deionized water was used to wash the given pale yellow powder, which was then dried at 80°C. Ultrasonic treatment was employed to prepare the N-TiO_2/g-C_3N_4 nanocomposite in order to disperse 25 wt.% of g-C_3N_4 in methanol and the addition of 75 wt.% of N-TiO_2 was done in the ultrasonic conditions for 30 min. Evaporation of methanol from the suspended solution was then followed under magnetic stirring at room temperature during 24 h.

3. Results and discussion

3.1. Characterization

X-ray diffraction (XRD) on Rigaku D/Max-2550pc as a powder diffract meter equipped with Cu Ka radiation (l¼0.1541 nm) was used to analyze the crystalline structure of the sample. The diffraction peak that appeared at 2θ = 27.7° was indexed as the (002) plane, corresponding to the interlayer stacking of the conjugated aromatic groups. The diffraction peak at around 2θ = 13.2° was characteristic of the in-plane structure of tri-s-triazine units and could be indexed as the (100) plane of g-C_3N_4 (Fig. 2 (Top)). Also, Fig. 2 (Bottom) reveals that there were several diffraction crystalline peaks indicating N-TiO_2.

The electron scanning electron microscopy (SEM) was employed to check the morphologies of the products (followed by Au coated by the sputtering method, using a coater sputter SC 761). The SEM images of the prepared nanocomposite are shown in Fig. 3. As can be seen, N-TiO_2/g-C_3N_4 had spherical nanosized particles.

3.2. Control test for the photocatalytic activity of N-TiO_2/g-C_3N_4 nanoparticles

In order to evaluate the photocatalytic activity of the prepared nanocomposite, the photolysis of dye (only in the presence of visible light without the photocatalyst), adsorption (in the presence of the photocatalyst and in the dark conditions), and photocatalytic removal of the dye were compared (Fig. 4). The negligible removal of the dye in dark and the absence of photocatalyst particles demonstrated that the adsorption and photolysis process did not contribute significantly to the dye removal.

3.3. Effect of the operational parameters on the photocatalytic removal of the dye

To investigate the effect of each parameter on the dye removal process, other parameters were kept constant in the selected values. The selected values for the experimental

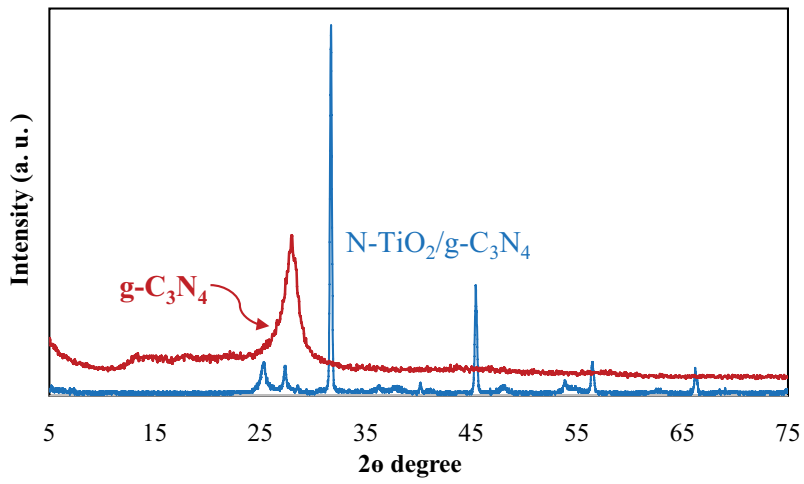

Fig. 2. XRD analysis of g-C_3N_4 (top) and N-TiO_2/g-C_3N_4 (bottom).

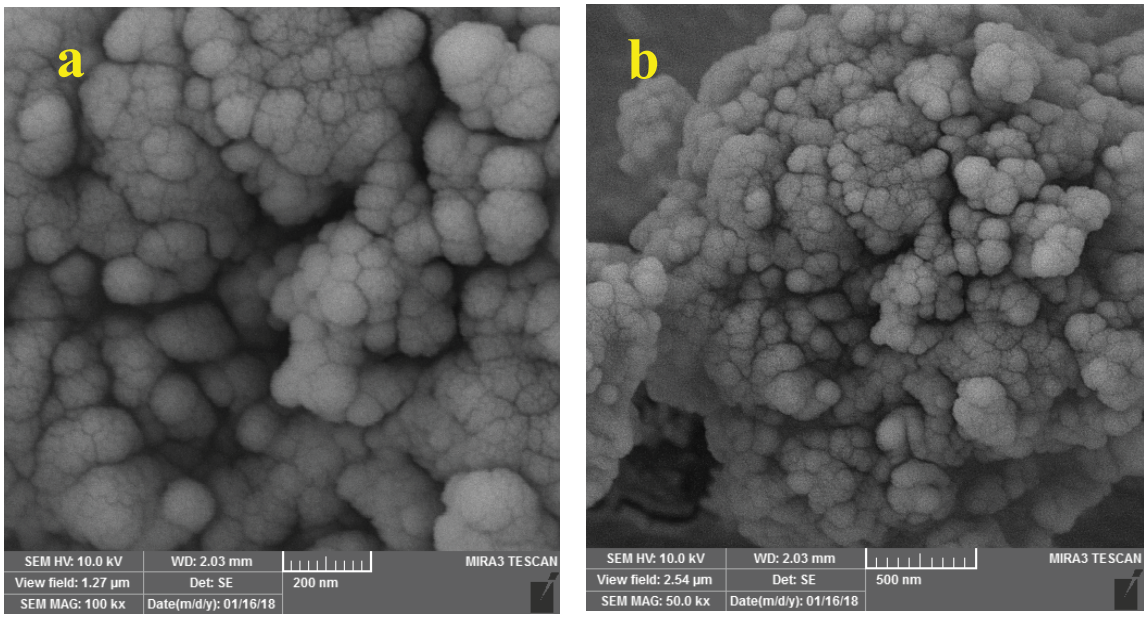

Fig. 3. (a and b) SEM images of synthesized N-TiO_2/g-C_3N_4 nanoparticles in different magnification.

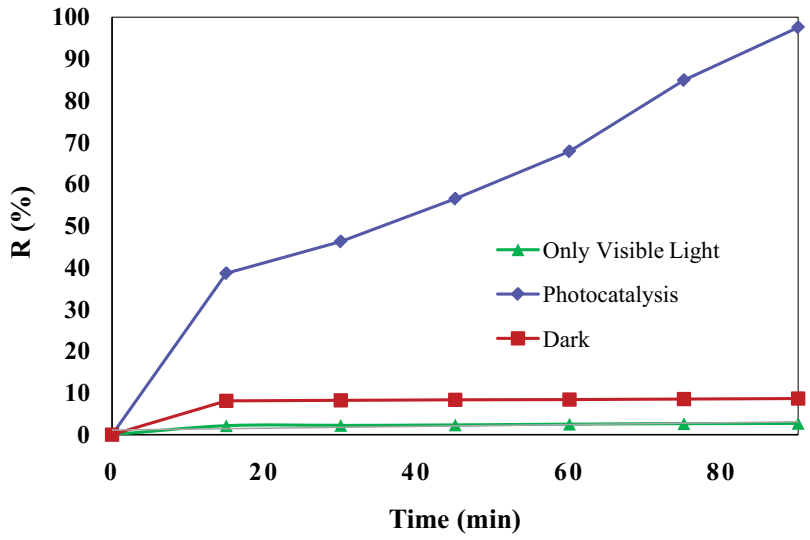

Fig. 4. Comparison of three processes in the removal of RO122. [RO122] = 10 mg/L, [Cat] = 120 mg/L, and pH = 6.

parameters were: photocatalyst dosage = 80, 90, 110, and 120 mg/L, dye concentration = 10, 12, 14, 18, and 20 mg/L, and pH = 4, 5, and 6.

3.4. Effect of the initial dye concentration

The effect of the dye concentration was investigated by varying the initial concentration from 10 to 20 mg/L while other parameters were kept in the selected values. The results showed that the removal efficiency of the dye was increased as the initial concentration of the dye was decreased (Fig. 5). This observation could be described by two different explanations. The first is the fact that at higher concentrations, the dye molecules can be adsorbed on the surface of the photocatalyst, covering all the active sites; this, in turn, could lead to a decrease in the removal efficiency. The second reason can be the adsorption of light photons by dye molecules, which could adversely affect the readiness of photons for starting the photocatalysis process [29,30].

3.5. Effect of the photocatalyst dosage

Fig. 6 illustrates the effect of the photocatalyst dosage (80, 90, 100, 120, and mg/L) on the degradation efficiency. The results showed that an increase in the photocatalyst dosage led to the rise of the removal efficiency, which could be attributed to the higher amount of the available active

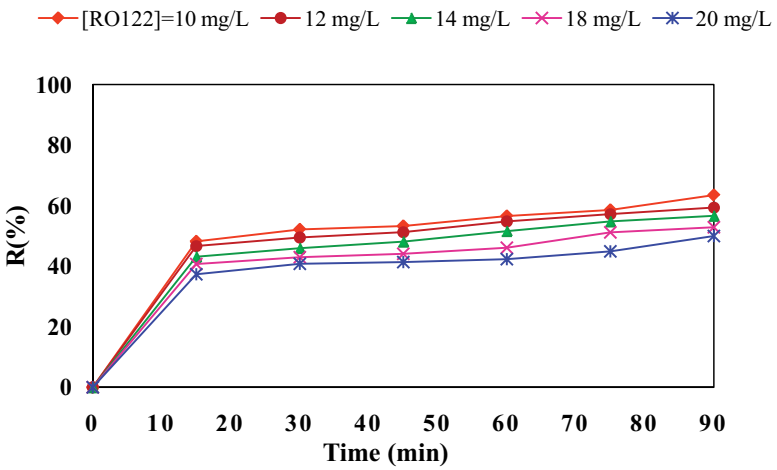

Fig. 5. Effect of initial dye concentration on removal degree. [Cat] = 120 mg/L and pH = 6.

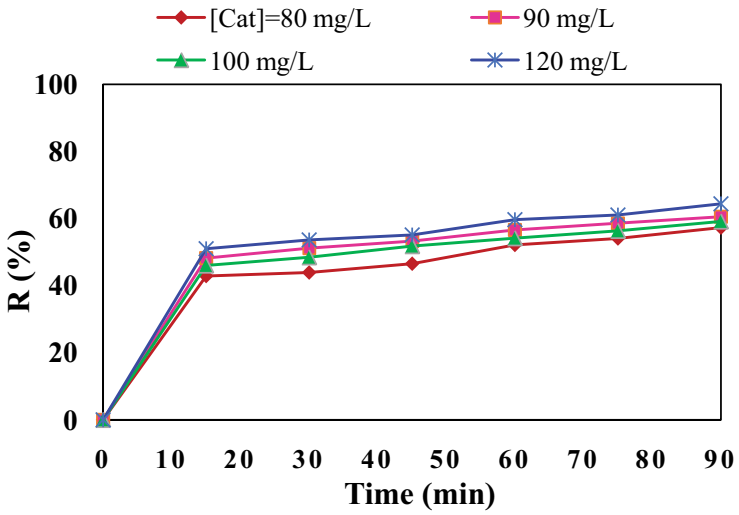

Fig. 6. Effect of photocatalyst dosage on removal degree [RO122] = 14 mg/L and pH = 6.

sites in the higher dosage of the photocatalyst. In particular, as the photocatalyst dosage was increased, the total active surface area was enhanced [24,39]. The photocatalyst dosage of 120 mg/L had the highest removal degree.

3.6. Effect of the initial pH of the dye solution

The effect of various pH values (4, 5, and 6) on the photocatalytic removal of the dye was examined. As can be seen from Fig. 7, the dye solution pH had a great impact on the removal efficiency, as the removal percentage was remarkably enhanced in the alkaline condition. The reason for this trend could be related to various factors such as the molecular structure of dye. In particular, RO122 is a cationic dye, so the insignificant removal in the acidic medium could be reasonable due to the electrostatic repulsion between the dye and the photocatalyst. At high pHs, due to the proliferation of OH^- in the solution, the repulsion force between OH^- and the photocatalyst surface could occur, thereby decreasing the production of OH radicals [40].

3.7. Modeling and optimization of the photocatalytic removal of the dye by ANN and GA

In the present research, MATLAB R2013a Neural Network Toolbox was used for modeling. The results obtained from 630 experimental data were applied to develop the neural network model. Features of the network are given in Table 1.

As the initial steps, the relationship between the independent variable (removal efficiency) and the dependent ones, namely, dye initial concentration, photocatalyst dosage, pH, and contact time, was modeled by ANN. In order to model the RO122 conversion in photocatalytic decomposition, the multi-input and single-output system with four inputs of the ANN model was developed.

The neural network, as a multi-layered perceptron, is commonly a parallel interconnected structure mainly composed of three different layers: (1) an input layer of the neuron (independent variables), (2) a number of hidden layers, and (3) an output layer (dependent variables). Determination of

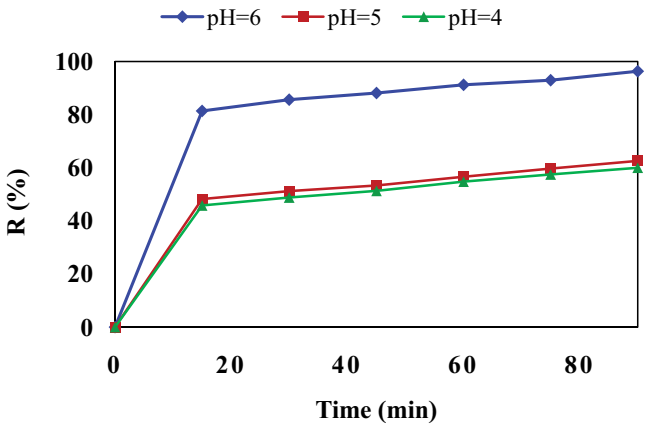

Fig. 7. Effect of pH on removal degree [RO122] = 14 mg/L and [Cat] = 120 mg/L.

the number of input and output layers is the main problem that should be modeled. The feature detector would be hidden layers with more than just one layer. Nevertheless, a single hidden layer with a large enough number of neurons can adequately interpret any input–output structure based on the universal approximation theory [41,42].

Variables such as the number of layers in the structure, the number of nodes in each layer, and the nature of the transfer functions might influence the topology of an ANN. So, the proper selection of input and output variable sets is important for successfully modelling the process by ANN. Modelling of a process is aimed at the optimization of the output responses. The next important step in the proceeding model is likely the optimization of the ANN topology. The selection of neurons in the hidden layer can reasonably have a remarkable effect on the performance of the network. Different numbers of neurons in the hidden layer, from 10 to 20, were thus tested in this work. The error function used in this study was the mean square error (MSE) (Fig. 8), which was calculated by the following equation in order to measure the performance of the network [43].

$$\mathrm{MSE} = \frac{1}{N}\sum_{i=1}^{N}\left(y_{i,\mathrm{pred}} - y_{i,\mathrm{exp}}\right)^2 \tag{5}$$

where N is the number of the data point, $y_{i,\mathrm{pred}}$ is the network prediction, $y_{i,\mathrm{exp}}$ is an experimental response, and i stands for an index of data.

In the present study, the initial concentration of the dye (mg/L), the photocatalyst dosage (mg/L), the initial pH of the dye solution, and contact time (min) were the feed input variables for the neural network. The degree of the dye removal (R%) was chosen as the output variable. The transfer function was also the sigmoidal transfer function in the hidden and output layers, which was the most widely used function, as given by Eq. (6):

$$f(x) = \frac{1}{1+\exp(-x)} \tag{6}$$

where $f(x)$ is the hidden neuron output. Train scaled conjugate gradient (trains) also served as the training function. A number of 624 experimental sets among the various data points were used to develop the ANN model.

To adjust the weight, the fundamental gradient descent algorithm was applied. It could modify the weights in the negative gradient, such that the performance function would decline very fast. This method, however, does not necessarily lead to the fastest convergence. The conjugate gradient method is an algorithm showing a faster convergence rate, as compared to the gradient descent algorithm. Hence, it is obvious that the cg methods are appropriate for the complicated neural networks.

Scaled conjugate gradient is called trains. The advantage of this method in comparison to other functions is that it does not need a line search algorithm per each iteration. Instead of line searching, mechanism of size scaling is used. Hence, even though trains algorithm needs more iteration for convergence, it will lead to quick answers, in comparison to other methods, such that the number of computations is remarkably decreased because per iteration [44].

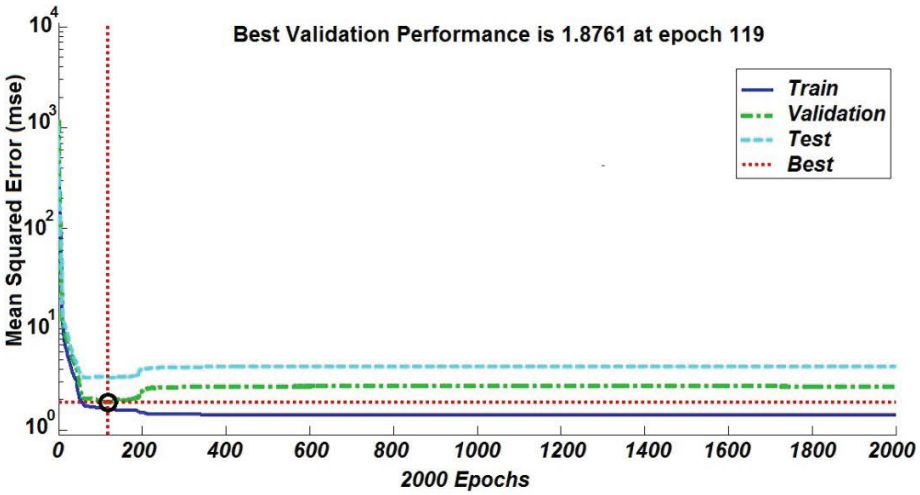

Fig. 8. MSE decreasing during the training of optimal ANN model for train, test, and validation data.

The samples were divided into three subsets of training, validation, and test groups, with 624, 600, and 600 samples, respectively. To investigate the validity and the modelling ability of the proposed model, validation, and test groups were randomly selected from the experimental data. Since the sigmoidal transfer function was used in the hidden layers, all the samples were scaled, ranging from 0.2 to 0.8. Hence, scaling all samples of the training, validation, and test sets (x_i) was done to a new value x_i by Eq. (7):

$$x_i = 0.2 + \frac{0.6\left(x_i\right) - \min\left(x_i\right)}{\max\left(x_i\right) - \min\left(x_i\right)} \tag{7}$$

where min (x_i) and max (x_i) are the extreme values of the input variables (x_i).

Calculation of training, validation, and test errors was then conducted by putting all outputs to an inverse range scaling in order to return the predicted responses to their original scale, as compared with the experimental responses. Fig. 9 compares the experimental data and the calculated values obtained by the neural network model having eight hidden layers. The reliability of prediction was assessed with the help of two lines: the perfect fit, where the predicted data was considered equal to the experimental data; it should be noted that all the data of an ideal model should lay on it, and the best fit of the data should be on a scatter plot. The correlation coefficient (R^2) of the latter is 0.997. In fact, better models have closer R^2 values to 1, thereby confirming that the neural network model could well simulate the photocatalytic degradation of RO122.

The optimization of the operational conditions for the photocatalytic degradation of RO122 was also conducted by the GA via MATLAB genetic algorithm function. To achieve the highest removal efficiency, the developed 4:20:1 ANN model was linked to GA to evaluate the function

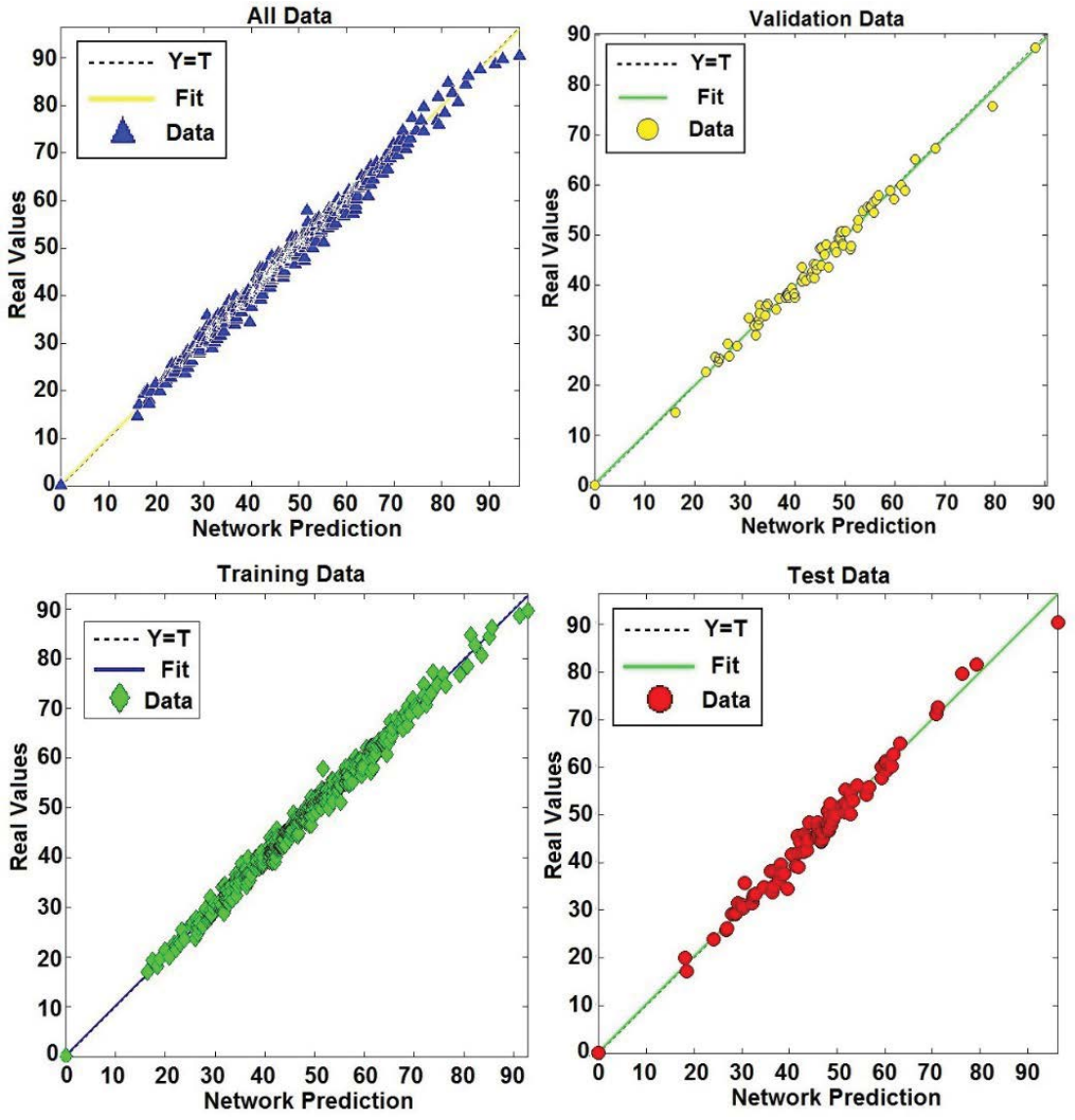

Fig. 9. ANN model prediction vs. experimental values for train, test, and validation data sets.

of GA, so that the optimal conditions would be created. In the given GA, each chromosome included four genes containing various numbers of bits according to variable precisions. The process of creating and decoding a random population of chromosomes with four genes was the initial step of the optimization process. GA randomly chose parents from the created population based on three rules of selection, crossover, and mutation. The selected parents were used to generate the children for the next generation. The initial population was developed toward the optimal conditions during consecutive generations. Table 1 demonstrates the proposed optimal operational parameters used to obtain the highest degradation efficiency. The proposed optimal conditions were then verified by a set of experiments. The maximum removal efficiencies were finally attained in the optimal amounts of variables in the experiments compatible with the predicted degradation efficiencies.

3.8. Mechanism of photochatalyst process

To further determine the mechanism of RO122 degradation, a radical trapping experiment was performed by adding radical scavengers such as isopropyl alcohol (IPA), disodium oxalate (OX), and 1,4-benzoquinone (BQ) to scavenge the hydroxyl, hole and super oxide radicals respectively in optimum value of parameters. As shown in Fig. 10a. All radical scavengers decreased the removal efficiency which confirmed the activities of radical types in removal of RO122. Accordingly, the more effective radicals in degradation process were $O_2^{-\bullet}$ and h^+. Fig. 10b shows the schematic electron and hole transfer mechanism to create reactive oxidative spices.

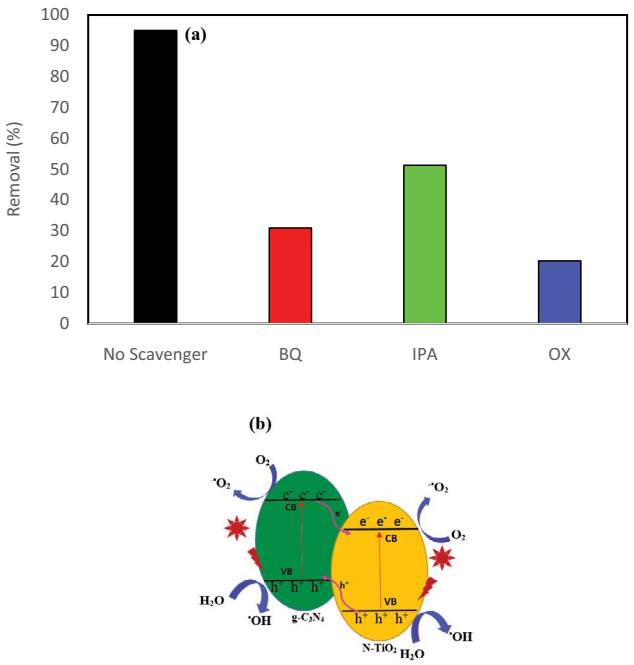

Fig. 10. (a) Effect of radical scavengers on the degradation of RO122 by photocatalysis process ($[RO122]_0$ = 10 mg/L, catalyst dosage = 120 mg/L, time = 90 min, and pH = 6) and (b) schematic representation of electron-hole transfer mechanisms.

4. Conclusion

The mixing of N-TiO_2 with g-C_3N_4 could lead to the modification of photoactivity. The concentration of the catalyst was also positively effective on the removal degree of dye, while the high pH value and the initial concentration of the dye were negatively proportional to it. The modeling and optimization of the photocatalytic removal of RO122 could be eventually fulfilled by the combination of the ANN-genetic algorithm with the desired nanocomposite.

Acknowledgments

This article is the result of Research project approved in the Isfahan University of Medical Sciences (IUMS). The authors wish to acknowledge to Vice Chancellery of Research of IUMS for the financial support, Research Project, #198342 and ethics code IR.MUI.RESEARCH.REC.1399.055.

References

[1] K.-J. Hwang, J.-W. Lee, W.-G. Shim, H.D. Jang, S.-I. Lee, S.-J. Yoo, Adsorption and photocatalysis of nanocrystalline TiO_2 particles prepared by sol–gel method for methylene blue degradation, Adv. Powder Technol., 23 (2012) 414–418.
[2] C. Wang, J. Zhu, X. Wu, H. Xu, Y. Song, J. Yan, Y. Song, H. Ji, K. Wang, H. Li, Photocatalytic degradation of bisphenol A and dye by graphene-oxide/Ag_3PO_4 composite under visible light irradiation, Ceram. Int., 40 (2014) 8061–8070.
[3] S. Adhikari, K. Sarath Chandra, D.-H. Kim, G. Madras, D. Sarkar, Understanding the morphological effects of WO_3 photocatalysts for the degradation of organic pollutants, Adv. Powder Technol., 29 (2018) 1591–1600.
[4] F. Mohammadi, B. Bina, M.M. Amin, H.R. Pourzamani, Z. Yavari, M.R. Shams, Evaluation of the effects of AlkylPhenolic compounds on kinetic parameters in a moving bed biofilm reactor, Can. J. Chem. Eng., 96 (2018) 1762–1769.
[5] A.M. Ghaedi, A. Vafaei, Applications of artificial neural networks for adsorption removal of dyes from aqueous solution: a review, Adv. Colloid Interface Sci., 245 (2017) 20–39.
[6] M.M.M.M. Amin, B. Bina, K. Ebrahim, Z. Yavari, F. Mohammadi, Biodegradation of natural and synthetic estrogens in moving bed bioreactor, Chin. J. Chem. Eng., 26 (2018) 393–399.
[7] C.M. Dominguez, N. Oturan, A. Romero, A. Santos, M.A. Oturan, Removal of lindane wastes by advanced electrochemical oxidation, Chemosphere, 202 (2018) 400–409.
[8] P. He, L. Song, S. Zhang, X. Wu, Q. Wei, Synthesis of g-C_3N_4/Ag_3PO_4 heterojunction with enhanced photocatalytic performance, Mater. Res. Bull., 51 (2014) 432–437.
[9] C.-S. Kim, B.K. Moon, J.-H. Park, S. Tae Chung, S.-M. Son, Synthesis of nanocrystalline TiO_2 in toluene by a solvothermal route, J. Cryst. Growth, 254 (2003) 405–410.
[10] W.S. Nam, G.Y. Han, Characterization and photocatalytic performance of nanosize TiO_2 powders prepared by the solvothermal method, Korean J. Chem. Eng., 20 (2003) 1149–1153.
[11] R. Djellabi, M.F. Ghorab, Solar photocatalytic decolourization of Crystal violet using supported TiO_2: effect of some parameters and comparative efficiency, Desal. Water Treat., 53 (2015) 3649–3655.
[12] N. Wang, Y. Zhou, C. Chen, L. Cheng, H. Ding, A g-C_3N_4 supported graphene oxide/Ag_3PO_4 composite with remarkably enhanced photocatalytic activity under visible light, Catal. Commun., 73 (2016) 74–79.
[13] J. Fan, Z. Zhao, W. Liu, Y. Xue, S. Yin, Solvothermal synthesis of different phase N-TiO_2 and their kinetics, isotherm and thermodynamic studies on the adsorption of methyl orange, J. Colloid Interface Sci., 470 (2016) 229–236.

[14] H. Irie, Y. Watanabe, K. Hashimoto, Nitrogen-concentration dependence on photocatalytic activity of $TiO_{2-x}N_x$ powders, J. Phys. Chem. B, 107 (2003) 5483–5486.
[15] J. Saien, Z. Mesgari, Highly efficient visible-light photocatalyst of nitrogen-doped TiO_2 nanoparticles sensitized by hematoporphyrin, J. Mol. Catal. A: Chem., 414 (2016) 108–115.
[16] M. Zafar, J.-Y. Yun, D.-H. Kim, Performance of inverted organic photovoltaic cells with nitrogen doped TiO_2 films by atomic layer deposition, Korean J. Chem. Eng., 35 (2018) 567–573.
[17] T. Yonar, G.E. Ustun, S.K. Akal Solmaz, Treatment of 3-indole butyric acid with solar photo-catalytic reactor, Desal. Water Treat., 48 (2012) 82–88.
[18] L. Ma, G. Wang, C. Jiang, H. Bao, Q. Xu, Synthesis of core-shell TiO_2@g-C_3N_4 hollow microspheres for efficient photocatalytic degradation of rhodamine B under visible light, Appl. Surf. Sci., 430 (2018) 263–272.
[19] M. Pelaez, N.T. Nolan, S.C. Pillai, M.K. Seery, P. Falaras, A.G. Kontos, P.S.M. Dunlop, J.W.J. Hamilton, J.A. Byrne, K. O'Shea, M.H. Entezari, D.D. Dionysiou, A review on the visible light active titanium dioxide photocatalysts for environmental applications, Appl. Catal., B, 125 (2012) 331–349.
[20] M.S. Nasr, M.A.E. Moustafa, H.A.E. Seif, G. El Kobrosy, Application of artificial neural network (ANN) for the prediction of EL-AGAMY wastewater treatment plant performance-EGYPT, Alexandria Eng. J., 51 (2012) 37–43.
[21] R. Mahesh, M. Gadekar, M. Ahammed, Modelling dye removal by adsorption onto water treatment residuals using combined response surface methodology-artificial neural network approach, J. Environ. Manage., 231 (2019) 241–248.
[22] K. Yetilmezsoy, S. Demirel, Artificial neural network (ANN) approach for modeling of Pb(II) adsorption from aqueous solution by Antep pistachio (*Pistacia Vera* L.) shells, J. Hazard. Mater., 153 (2008) 1288–1300.
[23] M.F. Ahmad, S. Haydar, A.A. Bhatti, A.J. Bari, Application of artificial neural network for the prediction of biosorption capacity of immobilized *Bacillus subtilis* for the removal of cadmium ions from aqueous solution, Biochem. Eng. J., 84 (2014) 83–90.
[24] A. Hassani, A. Khataee, M. Fathinia, S. Karaca, Photocatalytic ozonation of ciprofloxacin from aqueous solution using TiO_2/MMT nanocomposite: nonlinear modeling and optimization of the process via artificial neural network integrated genetic algorithm, Process Saf. Environ. Prot., 116 (2018) 365–376.
[25] M. Bagheri, S.A. Mirbagheri, Z. Bagheri, A.M. Kamarkhani, Modeling and optimization of activated sludge bulking for a real wastewater treatment plant using hybrid artificial neural networks-genetic algorithm approach, Process Saf. Environ. Prot., 95 (2015) 12–25.
[26] Y.R. Ding, Y.J. Cai, P.D. Sun, B. Chen, The use of combined neural networks and genetic algorithms for prediction of river water quality, J. Appl. Res. Technol., 12 (2014) 493–499.
[27] S. Bunsan, W.-Y. Chen, H.-W. Chen, Y.H. Chuang, N. Grisdanurak, Modeling the dioxin emission of a municipal solid waste incinerator using neural networks, Chemosphere, 92 (2013) 258–264.
[28] A. Aleboyeh, M.B. Kasiri, M.E. Olya, H. Aleboyeh, Prediction of azo dye decolorization by UV/H_2O_2 using artificial neural networks, Dyes Pigm., 77 (2008) 288–294.
[29] D.M. Himmelblau, Applications of artificial neural networks in chemical engineering, Korean J. Chem. Eng., 17 (2000) 373–392.
[30] A. Khani, B. Pezeshki, Easy simultaneous synthesis–immobilization of nanosized CuO–ZnO on perlite as a photocatalyst for degradation of acid orange 7 from aqueous solution in the presence of visible light, Desal. Water Treat., 57 (2016) 7047–7053.
[31] M.S. Seyed Dorraji, A.R. Amani-Ghadim, M.H. Rasoulifard, H. Daneshvar, B. Sistani Zadeh Aghdam, A.R. Tarighati, S.F. Hosseini, Photocatalytic activity of g-C_3N_4: an empirical kinetic model, optimization by neuro-genetic approach and identification of intermediates, Chem. Eng. Res. Des., 127 (2017) 113–125.
[32] A.R. Khataee, M. Fathinia, M. Zarei, B. Izadkhah, S.W. Joo, Modeling and optimization of photocatalytic/photoassisted-electro-Fenton like degradation of phenol using a neural network coupled with genetic algorithm, J. Ind. Eng. Chem., 20 (2014) 1852–1860.
[33] S. Azadi, A. Karimi-Jashni, S. Javadpour, Modeling and optimization of photocatalytic treatment of landfill leachate using tungsten-doped TiO_2 nano-photocatalysts: application of artificial neural network and genetic algorithm, Process Saf. Environ. Prot., 117 (2018) 267–277.
[34] M. Khajeh, A. Sarafraz-Yazdi, Z.B. Natavan, Combination of artificial neural network and genetic algorithm method for modeling of methylene blue adsorption onto wood sawdust from water samples, Toxicol. Ind. Health, 32 (2016) 437–446.
[35] N. Delgrange, C. Cabassud, M. Cabassud, L. Durand-Bourlier, J. Lainé, Neural networks for prediction of ultrafiltration transmembrane pressure – application to drinking water production, J. Membr. Sci., 150 (1998) 111–123.
[36] H. Demuth, M. Bwale, Neural Network Toolbox 5 User's, 2006.
[37] C. Sutherland, A. Marcano, B. Chittoo, Artificial Neural Network-Genetic Algorithm Prediction of Heavy Metal Removal Using a Novel Plant-Based Biosorbent Banana Floret: Kinetic, Equilibrium, Thermodynamics and Desorption Studies, M. Eyvaz, E. Yüksel, Eds., Desalination and Water Treatment, IntechOpen, London, UK, 2018, pp. 385–411.
[38] M.R. Zaki, J. Varshosaz, M. Fathi, Preparation of agar nanospheres: comparison of response surface and artificial neural network modeling by a genetic algorithm approach, Carbohydr. Polym., 122 (2015) 314–320.
[39] P. Devi, U. Das, A.K. Dalai, *In-situ* chemical oxidation: principle and applications of peroxide and persulfate treatments in wastewater systems, Sci. Total Environ., 571 (2016) 643–657.
[40] T.A. Kurniawan, L. Yanyan, T. Ouyang, A.B. Albadarin, G. Walker, $BaTiO_3$/TiO_2 composite-assisted photocatalytic degradation for removal of acetaminophen from synthetic wastewater under UV-vis irradiation, Mater. Sci. Semicond. Process., 73 (2018) 42–50.
[41] M.R. Sabour, A. Amiri, Comparative study of ANN and RSM for simultaneous optimization of multiple targets in Fenton treatment of landfill leachate, Waste Manage., 65 (2017) 54–62.
[42] D. Podstawczyk, A. Witek-Krowiak, A. Dawiec, A. Bhatnagar, Biosorption of copper(II) ions by flax meal: empirical modeling and process optimization by response surface methodology (RSM) and artificial neural network (ANN) simulation, Ecol. Eng., 83 (2015) 364–379.
[43] H. Karimi, M. Ghaedi, Application of artificial neural network and genetic algorithm to modeling and optimization of removal of methylene blue using activated carbon, J. Ind. Eng. Chem., 20 (2014) 2471–2476.
[44] B. Sharma, K. Venugopalan, Comparison of neural network training functions for hematoma classification in brain CT images, IOSR J. Comput. Eng., 16 (2014) 31–35.